SECM/15/089

Fatigue capacity of cold-formed steel roof battens under cyclic wind uplift loads

M. Kathekeyan[1] and M. Mahendran[1]

[1]Queensland University of Technology, Brisbane, Australia
E-Mail: myuran.kathekeyan@hdr.qut.edu.au, TP: +61 45075 4006
E-Mail: m.mahendran@qut.edu.au, TP: +61 73138 2543

Abstract: Steel roofs made of thin cold-formed steel roof claddings and battens are widely used in low-rise residential and industrial buildings all around the world. However, they suffer from premature localised pull-through failures in the batten to rafter connections during high wind events. A recent study proposed a suitable design equation for the pull-through failures of thin steel roof battens. However, it was limited to static wind uplift loading. In contrast, most cyclone/storm events produce cyclic wind uplift forces on roofs for a significantly long period, thus causing premature fatigue pull-through failures at lower loads. Therefore, a series of constant amplitude cyclic load tests was conducted on small and full scale roof panels made of a commonly used industrial roof batten to develop their S-N curves. A series of multi-level cyclic tests, including the recently introduced low-high-low (LHL) fatigue loading test, was also undertaken to simulate a design cyclone. Using the S-N curves, the static pull-through design capacity equation was modified to include the effects of fatigue. Applicability of Miner's rule was evaluated in order to predict the fatigue damage caused by multi-level cyclic tests such as the LHL test, and suitable modifications were made. The combined use of the modified Miner's law and the S-N curve of roof battens will allow a conservative estimation of the fatigue design capacity of roof battens without conducting the LHL tests simulating a design cyclone. This paper presents the details of this study, and the results.

Keywords: Cold-formed steel structures, Steel roofing systems, Thin steel roof battens, Wind action, Pull-through failures, Fatigue, Miner's rule

1. Introduction

Roofs made of thin and high strength cold-formed steel (CFS) claddings and battens are commonly used in low to medium-rise building construction. Such steel roof members are vulnerable to fatigue failures under high and fluctuating suction wind pressures. Particularly, low-pitched roofs of low to medium-rise buildings are subjected to high suction pressures and thus premature roof failures in high wind events, namely cyclones and storms.

Roofing assemblies comprise of claddings, battens/ purlin, rafter/ truss and their connections as shown in Figure 1. Generally, steel batten is a multi-span secondary structural member, spanning between roof trusses or rafters. The uplift wind pressure on roof claddings is transferred to the battens first through the cladding to batten connection, and then to rafter/truss via batten to rafter/truss connection. Finally, it is transferred to column and then to foundation as shown in Figure **1**.

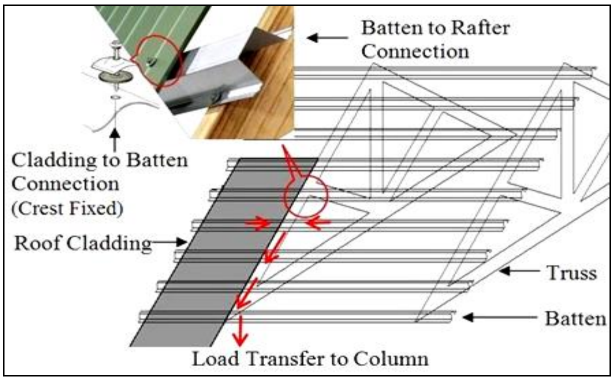

Figure 1: Typical roof structures and load path

Past cyclone damage studies have shown that roofs have mostly failed due to connection failures than member failures. They revealed that the cladding to batten and the batten to rafter screw connections shown in Figure 2 are the weakest links in the load transfer path. These connections can fail in two localised failure modes, namely static or fatigue failure depending on the wind event. Among them, the fatigue failure caused by cyclic loading is more critical as the fatigue failure capacity is about 40-50% of the static failure capacity [1].

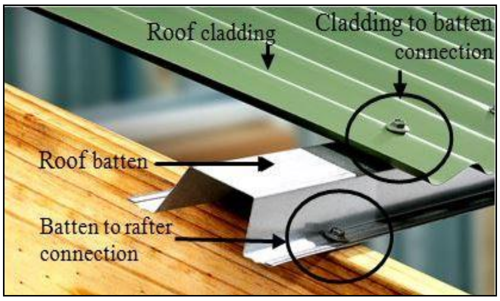

Figure 2: Critical roof connections

CFS roof members are susceptible to two types of local failures, namely, pull-through (Figure 3) and pull-out (Figure **4**) failures. A screw fastener head pulling through the cladding or batten under severe wind uplift pressure on the roof is referred to as pull-through failures whilst the same pulling out from the supporting member is referred to as pull-out failures. Therefore, a roof assembly can fail in one of the following four different failure modes during high wind events.

1. Pull-through and Pull-out failures of roof cladding to batten connection
2. Pull-through and Pull-out failures of roof batten to rafter connection

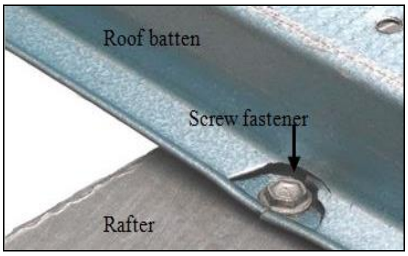

Figure 3: Pull-through failure of the batten to rafter connection

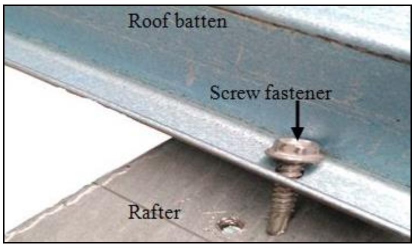

Figure 4: Pull-out failure of the batten to rafter connection

Many past studies have investigated all the possible failures associated with the cladding to batten connections, and improved the knowledge of this connection capacity under both static and cyclic wind effects. Such improvements made the batten to rafter connection the weakest connection in the roof assembly. A recent study investigated the static pull-through capacity of roof batten to rafter connections, and proposed suitable equations to predict the static pull-through capacity. However, the critical fatigue pull-through failure of roof batten to rafter connections has not been investigated. Therefore, this study investigates the fatigue pull-through failure of roof battens.

The failure at a connection progressively increases the loads on the adjacent fasteners, and leads to a complete collapse of building roofs. Therefore, a good knowledge of the fatigue behaviour and capacity of roof battens is essential. It can be achieved through the fatigue resistance curve (S-N curve in the form of stress/load level versus number of cycles to failure) obtained from constant amplitude cyclic tests. Such a S-N curve was obtained for an industrial roof batten through a series of constant amplitude cyclic tests. The batten and test assembly used were chosen to simulate real roofs in cyclone prone areas.

During cyclones, the amplitude of the cyclic wind uplift forces on the roof members is not constant. In order to include the varying amplitudes and the exposure period of roof members in a cyclone, a standard test method known as Low-High-Low (LHL) test was introduced. Such multi-level cyclic tests were also included in this study. Using constant amplitude and multi-level cyclic tests of roof battens, this study has investigated the fatigue pull-through capacity of roof battens when exposed to high wind events. This paper presents the details of this experimental study and the results.

2. Current Design and Test Methods

The Australian [3] and American standards [4] provides design formulae to calculate the pull-through capacity of mechanically fastened screw connections in tension. The design static pull-through capacity (ϕN_{ov}) based on [3] is as follows:

$$\phi N_{ov} = \phi\, 1.5\ t\ d\ f_u \qquad \text{for } 0.5 < t < 1.5 \text{ mm} \qquad (1)$$

Where, t is the thickness of the sheet in contact with the screw head, d is the greater of the screw head and the washer diameter (8 < d < 12.5 mm) and f_u is the specified ultimate tensile strength. It recommends the use of lesser of 90% of f_u for G550 steel sheet or 495 MPa for steel $0.6 < t < 0.9$ mm in thickness, and ϕ is the capacity reduction factor = 0.5. However, the applicability of Eq.1 to roof battens is questionable. Sivapathasundaram and Mahendran [5] showed that the pull-through capacities calculated form Equation (1) are much higher than the experimental results, ie. unsafe. The American cold-formed steel specification [4] also gives the same equation and is therefore not applicable to thin CFS battens.

Sivapathasundaram [6] developed the following design equations to predict the static pull-through capacity of roof battens. These equations predicted the pull-through capacities of roof battens used in their experimental study. However, they have not included the effects of cyclic wind loading in their equations.

For G550 steel roof battens:

$$F_{ov} = 8.68 t^2 f_u \tag{2}$$

and

For G300 steel roof battens:

$$F_{ov} = 2.96 t^{1.39} d^{0.61} f_u \tag{3}$$

European standard for CFS members and sheeting [7] recommends an equation to determine the fatigue pull-through capacity. The design pull-through capacity for screw connections subjected to cyclic wind loading is defined as follows:

Fatigue pull-through capacity = 0.5 x Static pull-through capacity (4)

Design static pull-through capacity
= t x d x f_u / γ_m (5)

Where, γ_m is the partial factor = 1.25, and others have been defined under Eq.1.

However, the design pull-through capacity of a 0.75 mm Grade 550 steel (ultimate tensile strength f_u is 700 MPa) batten fastened by 10 gauge screw fasteners (d = 11 mm) calculated from Equation (5) was 4.62kN, ie. 37% higher than the average static pull-through capacity (3.38 kN) of the batten tested by Sivapathasundaram and Mahendran [5]. Therefore both the static and fatigue capacity equations are not suitable to determine the pull-through capacity of thin CFS battens.

Due to the lack of design fatigue pull-through capacity equations, the current design practice is mainly based on laboratory experiments using a fatigue loading sequence known as Low-High-Low (LHL) pressure sequence [8]. This simulates the sustained fluctuating wind loading in a design cyclone using seven blocks of loading applied at a frequency less than 3 Hz (Table 1), where P_t is the ultimate limit state wind pressure on a roof due to the combined external and internal wind pressures.

Table 1: Low-High-Low pressure sequence [8]

Sequence	Number of cycles	Cyclic loads
A	4500	0 to 0.45 P_t
B	600	0 to 0.6 P_t
C	80	0 to 0.8 P_t
D	1	0 to 1.0 P_t
E	80	0 to 0.8 P_t
F	600	0 to 0.6 P_t
G	4500	0 to 0.45 P_t

3. Experimental Study

This experimental study consists of two phases. The first phase consists of constant amplitude cyclic tests, which included full scale roof tests followed by a series of small scale batten tests. The second phase consists of multi-level cyclic tests including LHL tests. A commonly used industrial roof batten and 10 gauge screw fasteners were used in these tests. It is made of 0.75 mm base metal thickness (BMT) G550 steel (minimum yield stress of 550 MPa) with 40mm height (
Figure **5**).

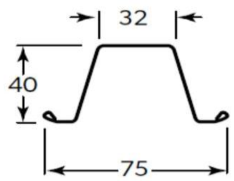

Figure 5: Test batten

3.1 Full Scale Tests

For research and test purposes, a two-span batten assembly is considered a satisfactory representation of multi-span batten assemblies used in buildings [9]. Therefore, a two-span roof batten assembly was chosen in the tests to simulate the fastener loads and the bending moment in the battens at the critical central support. 2.4 m x 1.5 m two-span roof panels were made using 0.48 mm BMT corrugated steel roof cladding, roof battens shown in Figure 5 and “C” purlins as shown in

Figure 6.

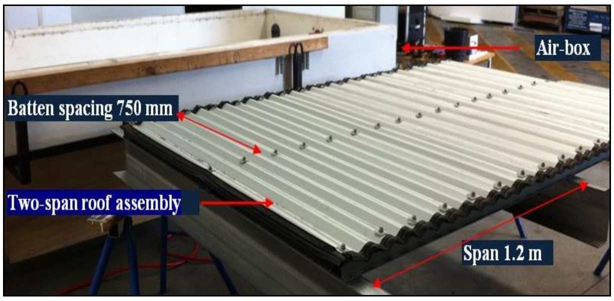

Figure 6: Full scale two-span roof assembly

Roof claddings were alternate crest fixed with battens using 6.5x55 self-drilling roofing screws with cyclone washers. 10 gauge self-drilling metal Tek screw fasteners were used to fix the battens to "C" purlins. Cyclone washers and roofing screws were selected to prevent local failures in the cladding to batten connections. In order to prevent the pull-out failures in the batten to rafter connections, Unbrako bolts and nuts were used instead of the 10g metal Tek screws in the critical central support of the middle batten, where the reaction force is the highest. A specially made screw head washer (head of 10g Tek screw) was used along with Unbrako bolts to simulate the metal Tek screw at the failure location (
Figure **7**). A constant torque 2.5N/m was used to install the bolt connections with lock nuts to prevent nut loosening during the cyclic tests.

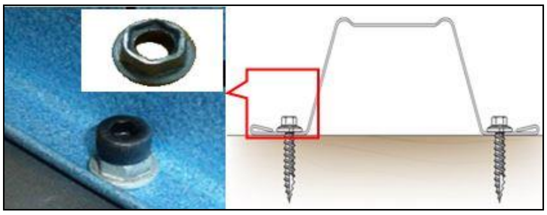

Figure 7: Simulated screw head washer

The roof panels were then tested in an air-box (
Figure **8**), where a wind suction pressure was simulated using a 7 kPa air pump and a controller. As seen in
Figure **8** the roof panels were placed upside down on top of the air-box. A special rubber seal was fixed around the roof panel to prevent air leak. Initially, three static tests were conducted. The suction pressure was slowly increased at a rate less than 15 N/s until complete pull-through failure occurred. The fastener loads were measured using 15 kN washer load cells (K-180) (
Figure **9**) to determine the static pull-through capacity.

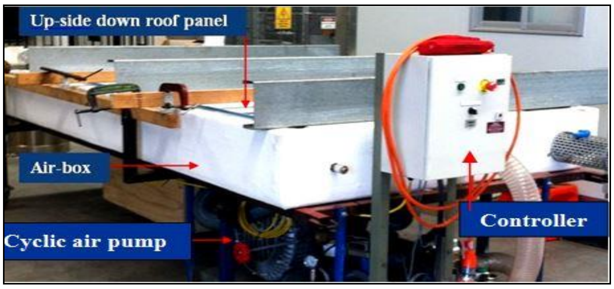

Figure 8: Full scale air-box test

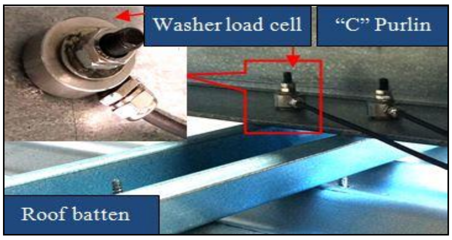

Figure 9: Washer load cells

A series of constant amplitude cyclic load tests was then conducted for different percentages of the measured static pull-through failure capacity to obtain the fatigue life (number of cycles to failure) of the roof batten. The air pump was controlled by a special air control valve to apply a sine wave form suction pressure on the roof test panels at a frequency of 1 Hz. The fastener tension load was measured using the washer load cells and the required cyclic pressures of each test were obtained by adjusting the air pressure based on the load cell reading.

3.2 Small Scale Tests

A series of small scale tests was included in this study to reduce the required number of full scale tests. Therefore, three different small scale battens (short, cantilever and two-span battens) were used to investigate the fatigue behaviour of roof battens. Figures 10 to 12 show the short, cantilever and two-span battens, respectively.

Among the small scale tests, initially a series of 150 mm long short batten tests (Figure 10) was conducted on a 100 kN MTS machine as was done for static pull-through capacity tests [5]. Although the batten's bending action was not simulated, it was included here to investigate the suitability of the previously used short batten tests and to investigate the effect of the absence of bending action on fatigue pull-through failures. Static and cyclic loads were applied by the MTS hydraulic actuator at the top flange of the batten until complete pull-through failure occurred. The static loading rate was 1mm/min while cyclic tests were conducted using force control at a frequency of 1 Hz.

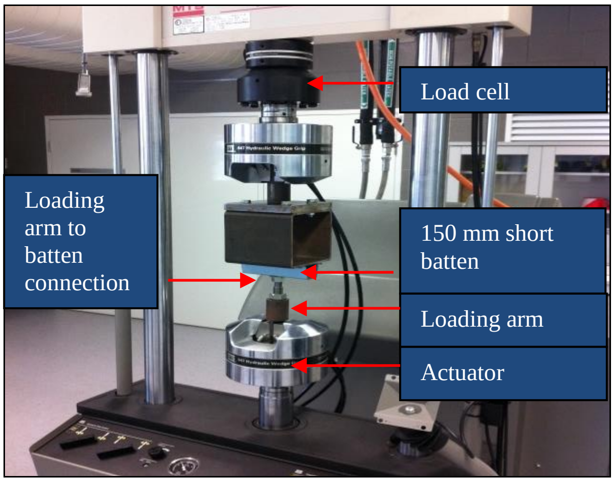

Figure 10: Short batten test

Secondly, a series of cantilever batten tests (Figure 11) was conducted by simulating both fastener tension load and bending moment in the batten. A 550 mm long cantilever batten (cantilever length of 240 mm) was used in this test series. The cantilever length was selected using simple bending theory to simulate the bending moment of the full scale roof assembly. Loading arm was bolted with the batten 240 mm away on either side of the connection as shown in Figure 11.

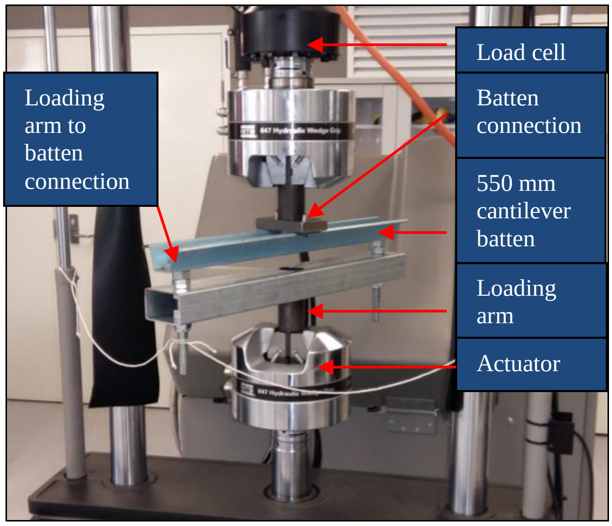

Figure 11: Cantilever batten test

Finally, a series of two-span batten tests was conducted on a 1900mm long batten (span of 900 mm) using a 500 kN hydraulic actuator (Figure 12). This test not only simulates the fastener tension load and the bending moment in the batten at the central support, but also the actual support conditions. The loading arm was bolted to the batten at its mid-span points. Batten span was calculated using simple bending theory to maintain the same fastener tension and bending moment in the batten at the central support of full scale panels. In these tests, the cyclic loads were applied as a sine wave at 1 Hz, and the number of cycles to failure was recorded. The load transferred to the critical central support connection (failure location) was measured using washer load cells.

In the cantilever and short batten tests, the load during the test was measured by the MTS load cell. However, in the air-box and two-span batten tests, two small washer load cells were used at the batten's central support, as shown in Figures 9 and 12, to measure the individual fastener reactions.

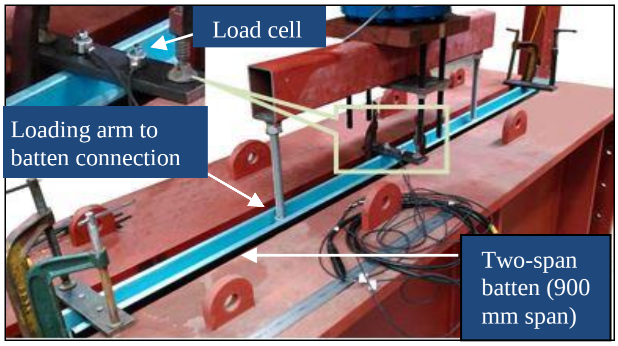

Figure 12: Small scale two-span batten test

3.3 Multi-level Cyclic Tests

The small scale two-span batten test method was used to conduct the multi-level cyclic tests with the same 1900 mm long two-span batten (span of 900 mm) and 10g screw fasteners to find the fatigue capacity of roof battens exposed to design cyclones, and to investigate the applicability of Miner's law. Cyclic tests of two-span battens were conducted at seven different percentages of P_t as required of the LHL test sequence (Table 1) [8]. The single load cycle D (Table 1) was held for 10 seconds at the ultimate design wind pressure, P_t [8]. Test was discontinued when the pull-through failure occurred.

4. Test Results and Comparison

4.1 Constant Amplitude Cyclic Tests

In order to produce the fatigue resistance curve (S-N curve) of the roof batten, static tests were first conducted using all the full scale and small scale tests, and their results are listed in Table 2. Figure 13 shows the average load per fastener versus displacement curve of the two-span batten test. The load increased up to a peak value (static pull-through capacity), which was mostly achieved when a tearing was initiated. After this, the load decreased until a complete pull-through failure occurred. The air-box tests were conducted in force control at a rate of 15 N/sec while all other tests were conducted in displacement control at a rate of 1mm/minute.

Table 2: Static pull-through capacity of roof batten

Test type	Static Capacity (kN)	Mean	COV
Air-box	3.06, 3.09, 3.61	3.25	0.10
Short batten	2.79, 2.94, 2.96, 3.01	2.93	0.03
Cantilever batten	2.76, 2.71, 2.93, 2.98	2.85	0.05
Two-span batten	3.00, 3.10, 3.12	3.07	0.02

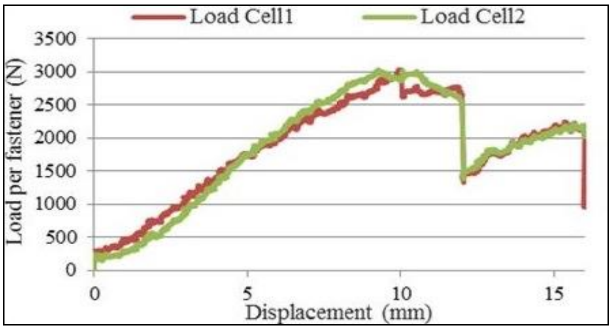

Figure 13: Average load per fastener versus displacement curves: two-span batten test

As seen in Table 2, the static pull-through failure capacities of roof battens obtained from short, cantilever and two-span batten tests agree reasonably well with the capacity obtained from the full scale air-box test. It should be noted that the air-box test was conducted in force control method, which generally gives a higher capacity compared to that obtained from displacement control tests. Also, a higher variation (COV = 0.1) was noticed in the large-scale tests due to the complex test arrangements. Due to the above reasons and as the variation between large and small scale tests are comparatively negligible, it can be concluded that all the small scale test methods can be used to obtain the static pull-through capacity of the roof battens. However, their applicability for the fatigue pull-through study is unknown. Therefore, constant amplitude cyclic load tests were conducted for a load range from zero to various percentages of the static pull-through capacity using all the test methods.

The number of cycles at crack initiation (N_i) as well as the number of cycles at the complete pull-through failure (N_f) were obtained and are listed in Table 3 to 6. In order to obtain N_i, displacement of the batten to rafter connection with respect to the loading point was recorded during the cyclic test. Such a displacement versus fatigue life graph is given in Figure 14. This graph can be divided into two segments, ie. up to the first notable peak (4500 cycles) followed by increasing displacement. In the first case, the displacement versus fatigue life graph is almost constant. From the first notable peak, where crack initiation occurred, the displacement increased in a manner as stable crack growth occurred. The two notable changes in the displacement indicate the crack initiation on the two sides of the batten. This pattern was noted in the majority of cyclic tests. Using this, cycles to crack initiation, N_i, were recorded in all the small scale tests, and are listed in Tables 4 to 6.

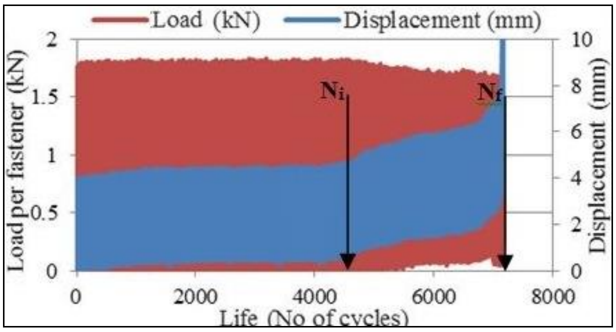

Figure 14: Force and displacement versus fatigue life graph of 56% cyclic test of two-span batten

Table 3: Constant amplitude cyclic test results - Full scale air-box tests

Applied load per fastener (kN)	Cyclic load (% of static pull-through load)	Number of cycles to failure
3.25	100	635
2.50	77	4753
2.20	68	3041
1.85	57	13100
1.60	49	21280
1.50	46	19581
1.50	46	19692
1.30	40	37781

Table 4: Constant amplitude cyclic test results - Two-span batten tests

Applied load per fastener (kN)	Cyclic load (% of static pull-through load)	Number of cycles to failure	
		N_i	N_f
3.07	100	1	308
2.73	89	1900	2400
2.39	78	2100	3000
2.05	67	3500	5372
1.71	56	4500	7162
1.54	50	5500	12290
1.26	41	26000	41617

Table 5: Constant amplitude cyclic test results - Cantilever batten tests

Applied load per fastener (kN)	Cyclic load (% of static pull-through load)	Number of cycles to failure	
		N_i	N_f
1.95	68.4	3100	5179
1.65	57.9	4400	6641
1.50	52.6	5400	13909
1.35	47.4	10000	20866
1.05	36.8	34000	47107

Table 6: Constant amplitude cyclic test results - Short batten tests

Applied load per fastener (kN)	Cyclic load (% of static pull-through load)	Number of cycles to failure	
		N_i	N_f
1.95	66.6	3200	6633
1.65	56.3	4800	11153
1.35	46.1	7500	28745

Constant amplitude cyclic test results were plotted as a S-N curve of cyclic pull-through failure load (percentage of static pull-through failure load) versus fatigue life (number of cycles to failure), and are presented in Figure 15. The S-N curves obtained from all the small scale tests agreed reasonably well with the S-N curve of the roof batten obtained from full scale air-box tests. This indicates that all the small scale tests can be used to study the fatigue behaviour of roof battens.

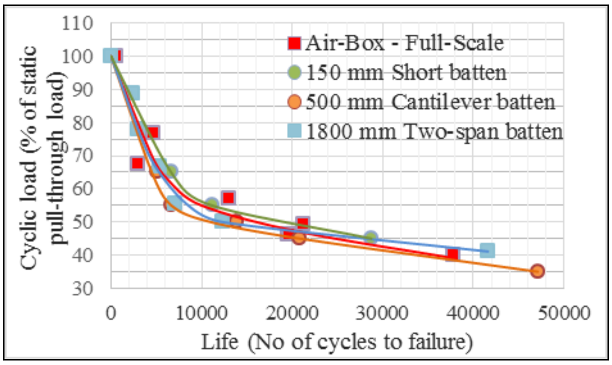

Figure 15: S-N curves of full scale and small scale tests for complete pull-through failure

Similarly, S-N curves for crack initiation, N_i, from all the small scale tests were compared as shown in Figure 16, which agreed perfectly well. As can be seen in Figures 15 and 16, both S-N curves clearly illustrate the reduction in fatigue life with increasing cyclic load levels. Also, it can be seen that below about 50 to 60% of the static pull-through capacity, fatigue life increment rate increases significantly. This indicates the presence of a fatigue limit in the range of 40 to 50% of the static pull-through failure load.

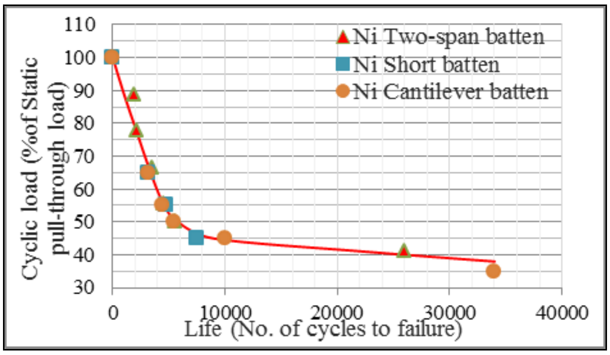

Figure 16: S-N curves of small scale tests for crack initiation

According to Figures 15 and 16, for a cyclic load closer to 40% of the static pull-through failure load, the roof batten will survive more than 25,000 cycles. However, in general, a house exposed to a cyclone will not experience such large numbers of cyclic loading. The LHL loading sequence [8] consists of about 10,000 cycles to represent a design cyclonic loading on a building roof. Therefore, by considering the damage caused by 10,000 cycles, a conservative fatigue limit of 45% of the static pull-through failure load can be proposed. However, it must be noted that real cyclonic loading is not constant amplitude cyclic loading. Therefore further guidance is needed.

Although all the small scale test results appear to agree reasonably well with the full scale test results, it is necessary to select the most suitable small scale test method for the fatigue study of roof battens. For this purpose, S-N curves obtained from each small scale test were compared with each other and full scale air-box tests. A good agreement between small scale two-span batten and full scale test results (Figure 17) reveal that the two-span batten test method can be used satisfactorily to simulate the full scale cyclic tests in the fatigue pull-through study of roof battens.

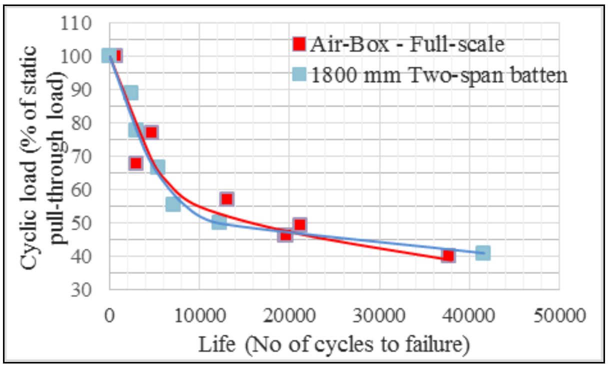

Figure 17: S-N curves of air-box and two-span batten tests for complete pull-through failure

Fatigue life (number of cycles to failure) from the cantilever batten test is always less than that obtained from the full scale test (Figure 18). This is because of the variation in the load at the critical failure connection (central support). The load applied to the batten to rafter connection in the cantilever batten test was constant throughout the test as shown in Figure 19, whilst the load in the critical central support connection in the air-box test reduced with fatigue damage as the load was transferred to the end supports with accumulated fatigue damage and associated changes to the connection fixity. This reflects the real case, i.e. load at the batten to rafter connections in roof varies with fatigue cracking during high wind events. This can only be simulated in two or more span batten tests. Therefore, small scale two-span batten test is the most suitable method for the fatigue study of roof battens.

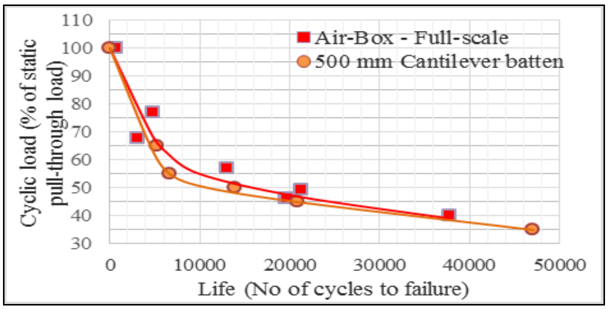

Figure 18: S-N curves of air-box and cantilever batten tests for complete pull-through failure

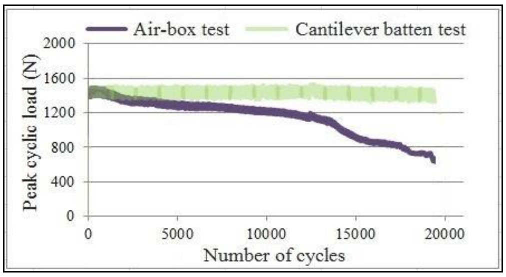

Figure 19: Peak cyclic load per fastener variation at the failure connection during cyclic loading

Although the short and cantilever batten tests do not simulate the actual condition, they can be compared to study the effect of bending due to two reasons: the load applied to the critical connection does not vary with fatigue damage, hence the fastener loads in these two tests are constant and equal; both tests used the same MTS machine, hence any machine error can be ignored. Therefore, S-N curves from these two test methods were compared as shown in Figure 20.

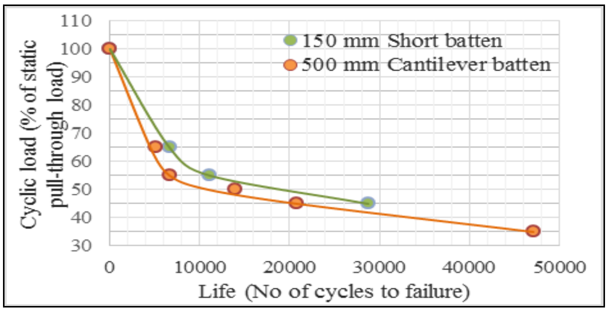

Figure 20: S-N curves of short and cantilever batten tests for complete pull-through failure

Table 7: Comparison of short and cantilever batten test results

Load applied per fastener (kN)	Cyclic load (% of static pull-through load)	Life (No of cycles to failure)		Variation %
		Cantilever batten test	Short batten test	
1.95	65	5179	6633	28
1.65	55	6641	11153	83
1.35	45	20866	28745	38

It shows a better fatigue performance in short batten tests compared to cantilever batten tests (Table 7). However, on the contrary, N_i obtained from these two tests agreed well. Figure 21 shows the comparison of N_i and N_f from these two test methods. It shows that the moment in the batten does not influence crack initiation; but it influences crack propagation. In other words, fastener tension load only influences the crack initiation, but both moment and fastener tension load at the critical support influence the crack growth and thus the complete pull-through failure, ie. the bending action influences N_f but not N_i. It must be noted that the variation between the fatigue life of the air-box and short batten tests is negligible as shown in Figure 15 as the S-N curve of the full scale air-box test is located between the S-N curves of short and cantilever batten tests.

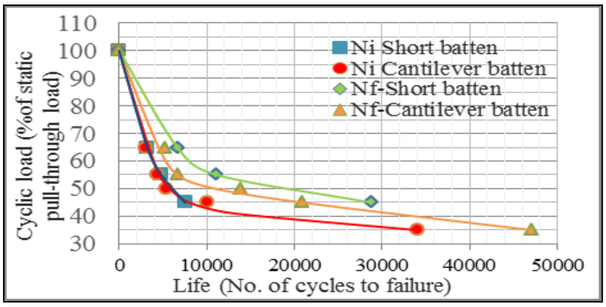

Figure 21: S-N curves of short and cantilever batten tests for crack initiation and complete pull-through failure

4.2 Multi-level Cyclic Tests

Table 8 lists the details of the multi-level cyclic tests of two-span battens conducted in this study and the results.

Table 8: Multi-level cyclic tests and the results

Test No	Pt (kN)	Pt*	Cyclic load sequences (% of P_t)			Cyclic load sequences *			No of cycles at each load sequence		
			A	B	C	A	B	C	A	B	C
T-1	3.07	100	70	80	70	70	80	70	1000	1500	1028
T-2	3.38	110	45	60	80	49.5	66	88	4500	600	295
T-3	3.53	115	45	60	80	51.8	69	92	4500	600	55
T-4	3.68	120	45	60	80	54	72	96	4500	600	80
T-5	4.45	145	45	60	--	65.3	87	--	4500	360	--

*- % of static pull-through failure load

Table 9: Fatigue damage calculated using the basic Miner's rule for Multi-level cyclic tests

Test No	Pt *	Cyclic load *	N applied	N_f failure	N_i failure	Damage-N_f	Damage-N_i
T-1	100	70	1000	4200	2850	1.03	1.49
		80	1500	2700	1900		
		70	1028	4200	2850		
T-2	110	49.5	4500	13600	6000	0.63	1.20
		66	600	5100	3300		
		88	295	1600	1100		
T-3	115	51.8	4500	10400	5200	0.62	1.14
		69	600	4400	3000		
		92	55	1100	700		
T-4	120	54	4500	9000	4700	0.81	1.41
		72	600	3900	2700		
		96	80	500	350		
T-5	145	65.3	4500	5200	3300	1.07	1.66
		87	360	1800	1200		
		--	0	0			

*- % of static pull-through failure load

The fatigue damage with respect to the complete pull-through failure was initially calculated using the basic Miner's rule as shown next.

$$F_t = \sum_{a=1}^{m} F_a = \sum_{a=1}^{m} \frac{n_a}{(N_f)_a} = 1 \qquad (6)$$

where F_t – Total fatigue damage, a ($1 \le a \le m$) – particular stress amplitude loading sequence, m - total number of various stress amplitude loading, F_a - fatigue damage for a particular stress loading, a, n_a - number of cycles applied in particular stress loading, a, and $(N_f)_a$ - total number of cycles to failure in the particular stress loading, a. Total number of cycles to failure, $(N_f)_a$, was obtained from the developed S-N curve (Figures 15 and 16) and the damage was calculated using Equation (6) for both crack initiation and complete pull-through failure. Table 9 presents the details and the damage results. Ideally, the calculated fatigue damage should be equal to one for a fatigue failure. However, it was less than one in some cases (T-2 to T-4), and are thus under-estimating the fatigue pull-through failure load. In contrast, the fatigue damage calculated for crack initiation is always greater than one. These results reveal that the basic Miner's rule does not always predict the fatigue damage accurately. Therefore, a modified Miner's rule for the total fatigue damage *(F_t)* is proposed as equal to the sum of damage up to crack initiation *(F_i)* and during crack propagation *(F_p)*.

$$F_t = F_i + F_p \qquad (7)$$

For a roof batten subjected to m number of various stress amplitude loading, a ($1 \le a \le m$), Equation 7 can be expanded as shown in Equations (8) to (10) for a crack initiation that occurred at x[th] stress amplitude loading, a=x, after y number of cycles.

$$F_t = \sum_{a=1}^{x+m} F_a = \sum_{a=1}^{x} F_a + \sum_{a=x}^{x+m} F_a = 1 \qquad (8)$$

$$\sum_{a=1}^{x} F_a = \frac{(N_{fi})_x}{(N_{ff})_x} \qquad (9)$$

$$\sum_{a=x}^{x+m} F_a = \frac{n_x - y}{(N_{ff})_x} + \sum_{a=x+1}^{m} \frac{n_a}{(N_{ff})_a} \qquad (10)$$

where,

N_{fi} and N_{ff} – Number of cycles to crack initiation and complete pull-through failure in a constant amplitude cyclic test at a given load level

n – Number of cycles applied at a given load level

In order to predict the fatigue damage using the modified Miner's rule, stress amplitude (x)

corresponds to crack initiation, $a=x$, and the number of cycles to crack initiation (y) at the x[th] load level, $n_x=y$, has to be found first. This can be achieved using Equation (11). The number of cycles to crack initiation (N_{fi}) and complete pull-through failure (N_{ff}) at a given load level can be obtained from the S-N curve obtained from constant amplitude cyclic tests. The S-N curves of the two-span batten test for crack initiation (N_{fi}) and complete pull-through failure (N_{ff}) are shown in Figure 22. **Error! Reference source not found.** presents the fatigue damage calculated using the modified Miner's rule.

$$\sum_{a=1}^{x-1} \frac{n_a}{(N_{fi})_a} + \frac{y}{(N_{fi})_x} = 1 \tag{11}$$

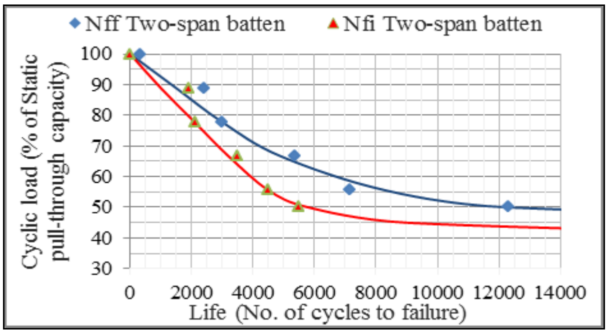

Figure 22: S-N curve of two-span batten test for crack initiation and complete pull-through failure

Table 10: Fatigue damage calculated using the modified Miner's rule for Multi-level cyclic tests

Test No	Cyclic load*	n_a	N_{ff}	N_{fi}	n_a/N_{fi}	y	$\frac{(N_{fi})_x}{(N_{ff})_x}$	Damage
T-1	70	1000	4200	2850	0.35	--		1.04
	80	1500	2700	1900	0.79	1233	0.70	
	70	1028	4200	2850	0.35	--		
T-2	49.5	4500	13600	6000	0.75	--		0.83
	66	600	5100	3300	0.18	--		
	88	295	1600	1100	0.27	75	0.69	
T-3	51.8	4500	10400	5200	0.87	--		0.78
	69	600	4400	3000	0.20	404	0.68	
	92	55	1100	700	0.08	--		
T-4	54	4500	9000	4700	0.96	--		0.98
	72	600	3900	2700	0.22	115	0.69	
	96	80	500	350	0.23	--		
T-5	65.3	4500	5200	3300	1.36	3300	0.63	1.07
	87	360	1800	1200	0.30	--		
	--	--	--	--	--	--		

*- % of static pull-through failure load

Fatigue damage predicted by both basic (
Table **9**) and modified miner's rules (**Error! Reference source not found.**) reveal that the modified Miner's rule (mean = 0.94, COV = 0.14) appears to better model the pull-through failure of the roof batten than the basic Miner's rule (mean = 0.83, COV = 0.26). Table 11 presents a summary of the predicted damage. The modified Miner's rule calculates the damage based on N_{fi} and N_{ff} values for the load level where the crack initiation occurred, thus ignoring any interactions/ damage up to that point. Further multi-level static tests are needed to verify this assumption.

Table 10: Comparison of damage predicted by basic and modified Miner's rules

Damage predicted	Predicted damage T-1	T-2	T-3	T-4	T-5	Mean	COV %
Basic	1.03	0.63	0.62	0.81	1.07	0.83	0.26
Modified	1.04	0.83	0.78	0.98	1.07	0.94	0.14

Finally, the fatigue capacity of the roof batten based on LHL loading sequence was obtained using the modified Miner's rule and validated through four LHL tests (Table 11). The ultimate design load, P_t, for fatigue pull-through failure (Table 1), was calculated using the modified Miner's rule based on Equation 11 and S-N curves for crack initiation. It was assumed that the fatigue pull-through capacity is based on the crack initiation at the end of sequence G. As seen in Table 12, the ultimate design load closer to crack initiation is 95% of the static pull-through capacity. Therefore, the design fatigue pull-through capacity of the tested roof batten can be taken as 95% of the batten's static pull-through capacity, i.e. 2.92 kN per fastener. Two LHL tests were conducted based on this P_t, which confirmed crack initiation at the end (Table 11). The load and displacement versus fatigue life graph in this test also confirms this observation (Figure 23).

Table 11: Low-High-Low (LHL) tests

Test No	P_t*	Sequences survived	Crack	Test status
LHL T-1	95	A-G	No	Pass
LHL T-2	95	A-G	Hairline crack	Pass
LHL T-3	100	A-G	Yes (Figure 24)	Failed
LHL T-4	115	A-C	Complete failure	Failed

Table 12: Fatigue damage for LHL Tests 1 and 2

A	$\%P_t$	n_a	P_t*	N_{fi}	F_a	$\sum_{a=A}^{G} F_a$
A	45	4500	42.75	15000	0.30	0.30
B	60	600	57.0	4300	0.14	0.44

C	80	80	76.0	2300	0.03	0.47
D	100	1	95.0	400	0.00	0.48
E	80	80	76.0	2300	0.03	0.51
F	60	600	57.0	4300	0.14	0.65
G	45	4500	42.75	15000	0.30	0.95

*- % of static pull-through failure load

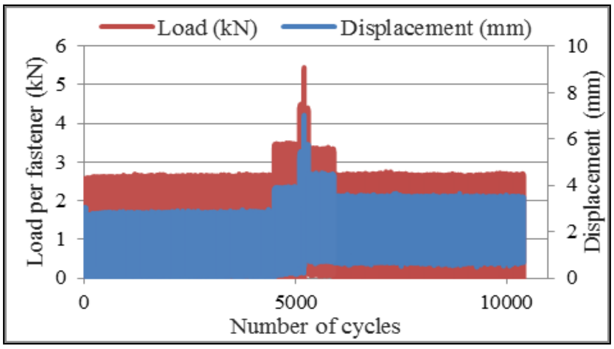

Figure 23: Fastener load and displacement versus fatigue life graph of 95% P_t LHL test

Table 12 shows that the design load that corresponds to a complete fatigue pull-through failure must be higher than 95% of the static pull-through capacity. However, a design load greater or closer to the static pull-through failure capacity should not be taken as the fatigue pull-through capacity as crack initiation dominated by static loading may occur closer to such a design load. To investigate this, two LHL tests were conducted, i.e. 100% (LHL T-3) and 115% (LHL T-4) of the static pull-through capacity to investigate the static failure at the single load sequence D and the fatigue failure before sequence D, respectively. These test results are given in Table 11. The LHL T-3 (closer to 100%) batten survived the LHL load sequences with minor crack as shown in Figure **24**.

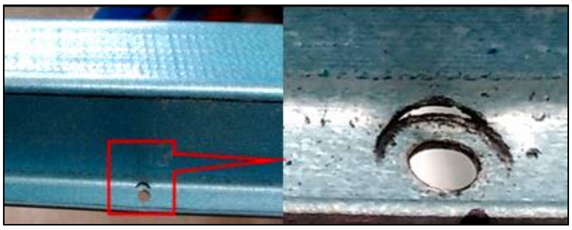

Figure 24: Crack pattern of 100% LHL test

The failure criterion given in [8] for roofing assemblies is that the tested roof assembly should not be disengaged from its supports during the LHL test. However, this will lead to a fatigue pull-through capacity of roof battens from LHL tests to be higher than its static pull-through capacity as observed in this study. This unusual observation is due to the fact that the static pull-through capacity is based on the first tearing of batten (when the load begins to drop) whereas the fatigue pull-through capacity is based on complete pull-through failure. The current failure criterion for LHL tests may only be adequate for roof sheeting due to the differences in the fatigue cracking modes of roof sheeting and battens. Further research is needed.

The small scale tests used in this study did not include the effects of the deformations of flexible supporting members, which might have accelerated the crack growth process and reduced the number of cycles to failure. In this case, LHL tests might give a lower fatigue pull-through capacity. However, based on the experimental results reported in this paper and the above discussions, the fatigue design pull-through capacity of 0.75 mm G550 roof battens exposed to a design cyclone (LHL test) can be taken as 2.92 kN per central support fastener, irrespective of their span as crack initiation does not depend on span (Figure 16).

5. Conclusions

This paper has presented the details of a series of constant amplitude and multi-level cyclic tests of an industrial roof batten to investigate the fatigue pull-through failures at the batten to rafter connection. Three different small scale constant amplitude cyclic tests along with full scale air-box tests were conducted to select the suitable small scale test method for the fatigue study of roof battens. Constant amplitude and multi-level cyclic test results based on the validated small scale two-span test method were then used to modify the basic Miner's rule to predict the fatigue damage in roof battens, and to find the fatigue pull-through capacity of roof battens exposed to a design cyclone simulated by the LHL test.

Test results and the modified Miner's rule have shown that the fatigue design pull-through capacity of roof battens exposed to a design cyclone can be conservatively estimated without conducting the more expensive and time consuming LHL tests. A similar approach used in this paper can be used for other roof battens. Alternatively, the use of a reduction factor of 0.45 with Equations 2 and 3 can be used as a very simple and conservative approach to allow for the fatigue effects of cyclonic wind loading.

Acknowledgements

The authors would like to thank Australian Research Council and Queensland University of

Technology (QUT) for the financial support for this research study. Thanks are also extended to all the technical officers at QUT's O-block laboratory and Banyo Pilot Plant Precinct for their support in using the required laboratory facilities.

References

[1]. Mahendran, M. (1989), Fatigue Behaviour of Corrugated Roofing under Cyclic Wind Loading, Technical Report No. 41, James Cook University CTS, Townsville.

[2]. Stephens, R.I., Fatemi, A., Stephens, R. R., Fuchs, H. O., (2000), Metal Fatigue in Engineering, John Wiley & Sons, Technology & Engineering, USA.

[3]. Standards Australia (2005), AS/NZS 4600, Cold-formed Steel Structures, Sydney.

[4]. American Iron and Steel Institute (AISI) (2007), North American Specification for the Design of Cold-Formed Steel Structural Members, Washington, DC, USA.

[5]. Sivapathasundaram, M., and Mahendran, M., (2014), Pull-through Failure Tests of Thin Steel Roof Battens under Wind Uplift Loads, Proc. of 22nd International Specialty Conference on Cold-Formed Steel Structures, St Louis, Mo, USA, pp. 679-696.

[6]. Sivapathasundaram, M. (2015), Localised Pull-through Failures of Thin Steel Roof Battens Subjected to Wind Uplift loads, Ph.D. thesis, Queensland University of Technology, Brisbane.

[7]. Eurocode 3(EN 1993-1-3). (2006), Design of steel structures - Part 1-3: General rules - Supplementary rules for cold-formed members and sheeting, Brussels

[8]. Building Code of Australia (BCA). (2008). Class 2 to 9 buildings, Vol. One and Class 1 & 10 buildings, Vol. Two, Sydney.

[9]. Standards Australia (1992), AS 4040.3, Methods of testing Sheet Roof and Wall Cladding - Resistance to Wind Pressures for Cyclone Regions, Sydney.